Tan, H.; Oishi, T.; Tanaka, A.; Doerffer, R.:

**Accurate estimation of the backscattering coefficient by light scattering at two backward angles**

In: Applied Optics (2015) Optical Society of America

DOI: 10.1364/AO.54.007718

# Accurate estimation of the backscattering coefficient by light scattering at two backward angles

**HIROYUKI TAN,[1,2,3,*] TOMOHIKO OISHI,[2] AKIHIKO TANAKA[2] ROLAND DOERFFER[3]**

[1]*Marine Engineering and Technology Service, Kitakyushu, Ohiraki 3-8-12, Fukuoka Ward, Kitakyushu city, Japan*
[2]*School of Marine Science and Technology, Tokai University, Orido 3-20-1, Shimizu Ward, Shizuoka city, Japan*
[3]*Institute for Coastal Research, Helmholtz-Zentrum Geesthacht, Max-Planck Strasse 1, D-21502 Geesthacht, Germany*
**Corresponding author: hiro@ko-marine.com*

**Backscattering coefficients are frequently estimated from light scattering at one backward angle multiplied by a conversion factor. We elucidated that the shape of the volume scattering functions (VSFs), particularly for scattering angles larger than 170°, cause significant variations in the conversion factor at 120°. Our approach uses the ratio of scattering at 170° and at 120°, which is a good indicator of the shape differences of VSFs for most oceanic waters and wavelengths in the visible range. The proposed method provides significant accuracy improvement in the determination of the backscattering coefficients with a prediction error of 3% of the mean.** 

## 1. Introduction

Optical properties of light scattering and absorption in waters are directly related to suspended biogeochemical constituents, such as phytoplankton and their associated materials (detritus) and inorganic compounds (minerals). The volume scattering function (VSF), denoted $\beta(\theta,\lambda)$, is an optical property of oceanic waters that is important to understand the radiative transfer of light fields in water [1], since it describes the light dispersion in all directions from an incident unpolarized beam. The total backscattering coefficient, $b_b(\lambda)$, is the integral of the VSF over scattering angle $\theta$ ranging from 90° to 180°. $b_b(\lambda)$ is also closely related to how scattered light leaves the sea surface [2]. Hence, a rigorous determination of $b_b(\lambda)$ is critical for accurate interpretation of remote sensing data (radiance measured by satellites) to get the biogeochemical properties of water, which are widely applied in understanding the earth environment, developing and running the climate forecast system, ecological modeling, fishing and human activities at sea, etc.

At present, however, the VSF is one of least-known optical properties of ocean water, due to practical difficulties in carrying out full VSF measurements according to its definition. Therefore, $b_b(\lambda)$ is also difficult to obtain. A different approach is typically applied to estimate $b_b(\lambda)$, in which light scattering measured at a single or at several backward angles is multiplied by a coefficient [3-12], the so-called fixed-angle approach. Oishi (1990) [3] first proposed this fundamental approach to estimate $b_b(\lambda)$. He found that the light backscattered at 120° was proportional to $b_b(\lambda)$. Maffione and Dana (1997) [4] recommended another scattering angle of 140° for the fixed-angle approach, introducing a non-dimensional constant, the conversion factor $\chi_t(\theta)$, for $b_b(\lambda)$. They pioneered an optical instrumental methodology for the fixed-angle approach, which is the basis of many instruments commercially available today (e.g. ECO BB sensors; Wet Lab, HydroScat Backscattering sensor; HobiLabs). Boss and Pegau (2001) [5] used the particulate VSF at scattering angles near 120° to estimate the particulate backscattering coefficient, $b_{bp}(\lambda)$ since scattering by pure seawater near this angle contributes little to $b_b(\lambda)$. In other words, the conversion factor of particles, $\chi_p(\theta)$, near 120° equals that of pure seawater. The currently applied fixed-angle approach relies on assumptions that (1) $\chi_p$ does not vary significantly over water types with respect to the optical properties and size distributions of suspended particles, and (2) $\chi_p$ is independent of wavelength, in the visible spectrum.

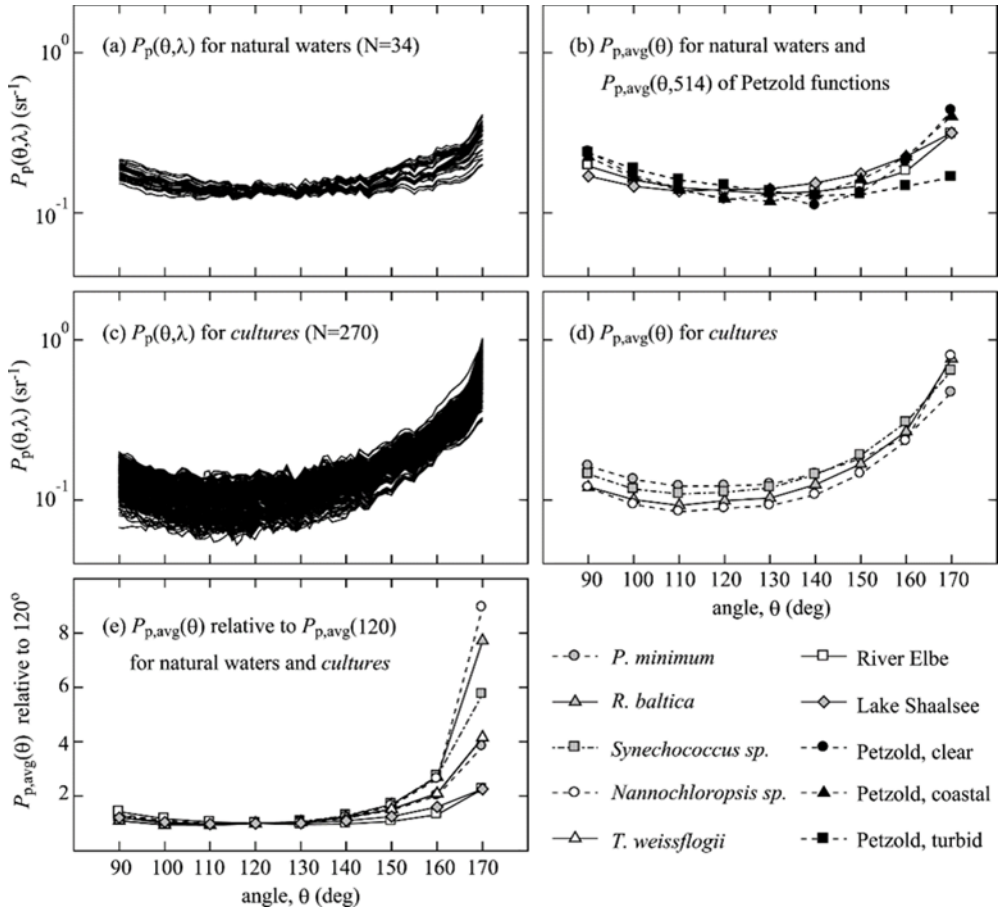


Fig. 1. $P_p(\theta,\lambda)$ in backward directions: (a) all $P_p(\theta,\lambda)$ for natural waters, (b) $P_{p,avg}(\theta)$ for natural waters compared to $P_{p,avg}(\theta,514)$ of Petzold VSFs at clear, coastal, and turbid oceans, (c) all $P_p(\theta,\lambda)$ for phytoplankton cultures, (d) $P_{p,avg}(\theta)$ for cultures, and (e) $P_{p,avg}(\theta)$ relative to 120° for the selected backward angles (10° steps) of all samples. Note that, the average for cultures are obtained from VSF data that includes all concentrations.

In recent years, several researchers have investigated VSFs in different bodies of seawater to find optimum values of and θ of $\chi_p$ for a more accurate estimations of $b_{bp}(\lambda)$, based on the above assumptions. For example, Sullivan and Twardowski (2009) [6] carried out numerous particulate VSF measurements for 658 nm wavelength light in a range of locations, from oceans to coastal waters. They concluded that assumption (1) regarding $\chi_p(\theta)$ scattering angles in the range of 110˚ to 120˚ are justified under most oceanic conditions. Berthon *et al.* (2007) [7] verified the relationship in the coastal northern Adriatic sea at 443, 490, 510, 555, 590, and 620 nm. They also confirmed that θ =120˚ is the most appropriate angle for the derivation of $b_{bp}(\lambda)$, as opposed to θ=140˚. Furthermore, Zhang *et al.* (2014) [8] recently reported that the minimum variation in conversion factor occurs around θ=120˚, based on field observations in the US and theoretical analysis. However, there is still an open question concerning whether $\chi_p(\theta)$ is constant in different conditions of oceanic water, such as in phytoplankton blooms. In 1996, Jodai *et al.* [9] first demonstrated that the fixed-angle approach might lead to significant error in the estimate of $b_{bp}(\lambda)$ in the presence of phytoplankton cultures. Chami *et al.* (2006) [10] presented a remarkable conclusion that a significant spectral dependence of $\chi_p(140)$ is found for phytoplankton cultures, while $\chi_p$ at this angle for the Black sea is wavelength independent. As a consequence, the average error in the estimates of $b_{bp}(\lambda)$ using a constant value of $\chi_p(140)$=1.18 over 443, 490, and 555 nm is found to be 7% for the Black sea and 26% for algal cultures. Contrary to the previous results, Whitmire *et al.* (2010) [11] found a spectrally independent function of $\chi_p(\theta)$ for phytoplankton cultures at several backward angles. Therefore, $\chi_p(\theta)$ should not be assumed to be constant in all types of waters and wavelength, as pointed out by Chami *et al.* (2006) [10]. This suggests that careful attention is required before making any assumptions about $\chi_p(\theta)$, which is very inconvenient in practical situations. Although Freda (2012) [12] recently presented the spectral shape formula of the conversion factor at 140˚ at the southern Baltic sea, he concluded that the relation probably cannot be universally applied to different types of oceans. Chami *et al.* (2006) [10] also pointed out the difficulty in devising a systematic law describing the spectral dependence of the conversion factor in a simple manner that is adaptable to all oceanic waters.

Our main objective in this study is to improve the fixed-angle approach to estimating $b_{bp}(\lambda)$ and $b_b(\lambda)$ by overcoming the problems mentioned above. In section 2, we briefly describe an original VSF meter and the samples used in this study. In section 3, VSFs measured with our VSF meter are analyzed and compared with existing data. We present $\chi_p(\theta)$ calculated using our VSF data by the same methods as previous studies to confirm the conclusions of various researchers. In section 4, we introduce an alternative conversion factor for accurate estimation of $b_{bp}(\lambda)$, which solves the problems of the currently applied fixed-angle approach. In section 5, we discuss the testing of the performance of our fixed-angle approach in different types of waters and wavelengths using VSFs of other researchers, Lorenz-Mie computations, and our measured data. Finally, in section 6, we summarize the results of our fixed-angle approach, which provides significantly more accurate the estimate of $b_b(\lambda)$.

## 2. Spectral VSF measurements and samples

The VSF is defined as [13]:

$$\beta(\theta,\lambda) = dI(\theta,\lambda)/E(\lambda)\,dv, \quad \textbf{(1)}$$

where $E(\lambda)$ is the incident irradiance on the scattering volume, $dv$, and $dI(\theta,\lambda)$ is the intensity of the light scattered by $dv$ in a direction θ away

from the incident beam, which has wavelength λ. The VSF of suspended particles is obtained simply by subtraction of scattering by pure seawater, i.e., $\beta_p(\theta,\lambda)=\beta(\theta,\lambda)-\beta_{sw}(\theta,\lambda)$. The backscattering coefficient by suspended particle is determined by integrating $\beta_p(\theta,\lambda)$ over the backward hemisphere, where the scattering angle ranges from 90° to 180°, as [13]:

$$b_{bp}(\lambda) = 2\pi\int_{\pi/2}^{\pi}\beta_p(\theta,\lambda)\sin\theta d\theta. \quad \textbf{(2)}$$

Therefore, $b_b(\lambda)=b_{bp}(\lambda)+b_{bsw}(\lambda)$.

VSFs in the visible spectrum were collected with a prototype of an imaging Volume Scattering Function Meter, iVSFM, developed by the Helmholtz-Zentrum Geesthacht (HZG), Geesthacht, Germany. Briefly, the iVSFM can determine VSF of scattering angles from 8° to 172° simultaneously as an image picture with a cooled CCD camera; Tan *et al*. (2013) [14] provide a more detailed description of the iVSFM construction, operating system, corrections and calibration, etc. The iVSFM has angular resolution of 1° and made measurements for λ from 400 to 700 nm at 20 nm intervals, while blocking fluorescence emission by suspended particles for measurements of λ<480 nm. To correct for attenuation in the measured scattered light intensity, the beam attenuation coefficient was measured by a standard attenuation meter using purified distilled water (MilliQ water) as a standard [13]. The uncertainty in the VSF measurement was evaluated as the standard error of 20 scattering measurements at 90° of MilliQ water, which is regarded as the smallest scatter in nature. The highest error is <15% of the scattered measurement value. $\beta_p(\theta)$ was obtained by subtracting $\beta_{sw}(\theta)$ from measured $\beta(\theta)$ [15]. To determine $b_{bp}(\lambda)$, the missing VSFs in extreme back direction (173°-180°) were linearly extrapolated on a log-scale.

304 VSFs datasets were used in our analysis, including datasets from natural waters (number of data sets N=34), specifically, shore waters (very turbid) of River Elbe, and Lake Shaalsee in Germany; and cultures of five phytoplankton (N=270), *Prorocentrum minimum*, *Rhodomonas baltica*, *Synechococcus sp.*, *Nannochloropsis sp*., and *Thalassiosira weissflogii*. For each culture, we collected VSF data from different concentrations to determine the specific VSF (results to be published soon). All cultures were provided by the Alfred-Wegener Institute for Polar and Marine Research, Germany, and maintained in 12 hours light cycles in their exponential growth phase by daily dilution with F/2 water. For reference, the beam attenuation magnitudes in the samples are presented in Appendix B.

## 3. Analysis of $\beta_p(\theta,\lambda)$ and $\chi_p(\theta)$ compared with previous studies

### A. The shape variation of $\beta_p(\theta,\lambda)$

The phase function due to particulate matter, $P_p(\theta,\lambda)$ ($sr^{-1}$), is often used in discussions of the shape variability of $\beta_p(\theta,\lambda)$, and is defined as $\beta_p(\theta,\lambda)$ normalized by $b_{bp}(\lambda)$:

$$P_p(\theta,\lambda) = \beta_p(\theta,\lambda)/b_{bp}(\lambda). \quad \textbf{(3)}$$

Figure 1a shows a dataset of $P_p(\theta,\lambda)$ of natural waters for all wavelengths measured. Minimum values and shape variance of $P_p(\theta,\lambda)$ for natural waters occur around 120°, i.e., $P_{p,avg}(\theta)$, averaged $P_p(\theta,\lambda)$, over all natural waters at 120° is 0.14 with 5% relative standard deviation, σ*, which is the standard deviation of σ relative to the mean value (hereafter denoted as mean ± σ* in %). Larger values and variations σ* of $P_{p,avg}(\theta)$ of natural waters occur towards angles of 90° and 170°, i.e., $P_{p,avg}(90)$=0.18±9% and $P_{p,avg}(170)$=0.31±18%, respectively. These angular variability trends are reasonably consistent with Sullivan and Twardowski (2009) [6] for $P_{p,avg}(\theta,658)$ of not only *in situ* measurements, but also calculations using the Fournier-Forand phase function [16] (see Fig. 3b in their study). VSFs measured by Petzold [17] are frequently used in studies of marine optics as representative VSFs of seawater. Fig. 1b shows the comparison of $P_{p,avg}(\theta)$, $P_p(\theta,\lambda)$ averaged over measured wavelengths, for natural waters, to $P_{p,avg}(\theta,514)$ of Petzold functions in three different water types: clear, coastal and turbid oceans. As shown in the figure, the shape of our $P_{p,avg}(\theta)$ is roughly similar and comparable to $P_{p,avg}(\theta,514)$ of Petzold functions. $P_{p,avg}(\theta)$ of our natural waters intersect at 115° with $P_{p,avg}(\theta,514)$ of clear and coastal waters from Petzold study, and around 120°-130° with $P_{p,avg}(\theta,514)$ of turbid water. Combining our data with $P_p(\theta,514)$ of Petzold study, the minimum variability of σ* occurs around 129° at 5%. Fig. 1c shows $P_p(\theta,\lambda)$ of five cultures of phytoplankton for all concentrations and wavelengths measured. Compared with natural waters. Larger shape variances of $P_p(\theta,\lambda)$ (σ*>13%) are confirmed for all backward directions; the minimum σ* occurs around 150° at 13% and the maximum occurs around 170° at 26%. The dataset shown in Fig. 1d is $P_{p,avg}(\theta)$ for individual phytoplankton cultures. Note that, for cultures, $P_{p,avg}(\theta)$ was obtained from VSF data that includes all concentrations of phytoplankton measured in this study. The maxima of $P_{p,avg}(\theta)$ for all cultures are commonly found at 170° with significant increases of a factor of over 2 from the minima at 120°, i.e., $P_{p,avg}(170)$=0.31 to 0.79, while $P_{p,avg}(120)$=0.08 to 0.12. Since the minimum of scattering for both natural waters and cultures frequently appeared around 120°, we normalize all of $P_{p,avg}(\theta)$ by $P_{p,avg}(120)$. As shown in Fig. 1e, the shape of $P_{p,avg}(\theta)$ relative to 120° depends on the type of waters, especially for cultures. Further, the differences between $P_{p,avg}(\theta)$ and $P_{p,avg}(120)$ appear most extreme at backward angles around 170°. For instance, $P_{p,avg}(170)/P_{p,avg}(170)$ for all natural waters are quite consistent at 2.3, whereas that ratio for cultures of phytoplankton varies from 3.8 to 8.9. In other words, the ratio at these angles seems to be a good indicator of shape differences in VSFs, as we will discuss in section 4.

Fig. 2. Angular variation of $\chi_{p,avg}(\theta)$ for (a) natural waters, and (b) cultures of phytoplankton. The star symbols are the means of $\chi_p$ in the literature at 120° and 140°, $\chi_{p,mean}(120)$=1.18 and $\chi_{p,mean}(140)$=1.25, respectively (see Appendix C). Note that the means for cultures are obtained from VSFs for all wavelengths and all concentrations measured in this study.

### B. Particulate conversion factor for $b_{bp}(\lambda)$

$b_{bp}(\lambda)$ is obtained by integrating measured $\beta_p(\theta,\lambda)$ over the backward hemisphere (see. Eq. 2). Measuring the VSF for the whole hemisphere is time-consuming and requires a complicate system. Thus, it is currently not practical to use VSF meter in the fields. Alternatively, $b_{bp}(\lambda)$ can be estimated from the measured scattering at selected angles and multiplying by an appropriate scaling factor. The rigorous expression of the fixed-angle approach is shown as:

$$b_{bp}(\lambda) = 2\pi\varphi_p(\theta,\lambda)\beta_p(\theta,\lambda), \quad \textbf{(4)}$$

**Table 1. Average and σ* of $\chi_p(\theta)$ for individual samples, natural waters, and cultures at selected backward angles. N is number of [illegible] standard deviation normalized by the mean.**

| 100˚ | 110˚ | 120˚ | 130˚ | 140˚ | 150˚ | 160˚ | 170˚ |
|---|---|---|---|---|---|---|---|
| 0.99 | 1.11 | 1.16 | 1.21 | 1.17 | 1.08 | 0.88 | 0.54 |
| 5.7 | 4.8 | 3.7 | 2.7 | 2.5 | 4.2 | 8.9 | 23.6 |
| 1.09 | 1.17 | 1.14 | 1.13 | 1.04 | 0.91 | 0.71 | 0.52 |
| 5.7 | 4.7 | 4.9 | 3.7 | 2.6 | 5.3 | 10.5 | 17.8 |
| 1.19 | 1.31 | 1.30 | 1.27 | 1.10 | 0.88 | 0.65 | 0.34 |
| 8.5 | 7.1 | 5.9 | 5.3 | 5.7 | 7.5 | 7.9 | 12.0 |
| 1.63 | 1.78 | 1.64 | 1.57 | 1.28 | 0.96 | 0.60 | 0.22 |
| 16.7 | 18.3 | 13.9 | 11.1 | 8.3 | 8.8 | 9.1 | 22.4 |
| 1.39 | 1.48 | 1.44 | 1.35 | 1.12 | 0.84 | 0.53 | 0.25 |
| 13.9 | 11.3 | 10.8 | 11.1 | 9.7 | 8.7 | 9.0 | 12.4 |
| 1.76 | 1.96 | 1.88 | 1.79 | 1.51 | 1.12 | 0.69 | 0.21 |
| 16.8 | 18.4 | 19.8 | 17.6 | 15.3 | 14.6 | 11.0 | 22.3 |
| 1.37 | 1.39 | 1.30 | 1.23 | 1.06 | 0.85 | 0.62 | 0.32 |
| 9.6 | 9.0 | 8.1 | 4.9 | 4.4 | 6.5 | 9.4 | 19.2 |
| 1.04 | 1.14 | 1.15 | 1.17 | 1.11 | 1.00 | 0.80 | 0.53 |
| 7.4 | 5.4 | 4.3 | 4.6 | 6.8 | 9.9 | 14.1 | 20.9 |
| 1.47 | 1.58 | 1.51 | 1.44 | 1.22 | 0.93 | 0.62 | 0.27 |
| 19.8 | 21.6 | 20.3 | 18.9 | 17.4 | 15.0 | 13.0 | 26.8 |

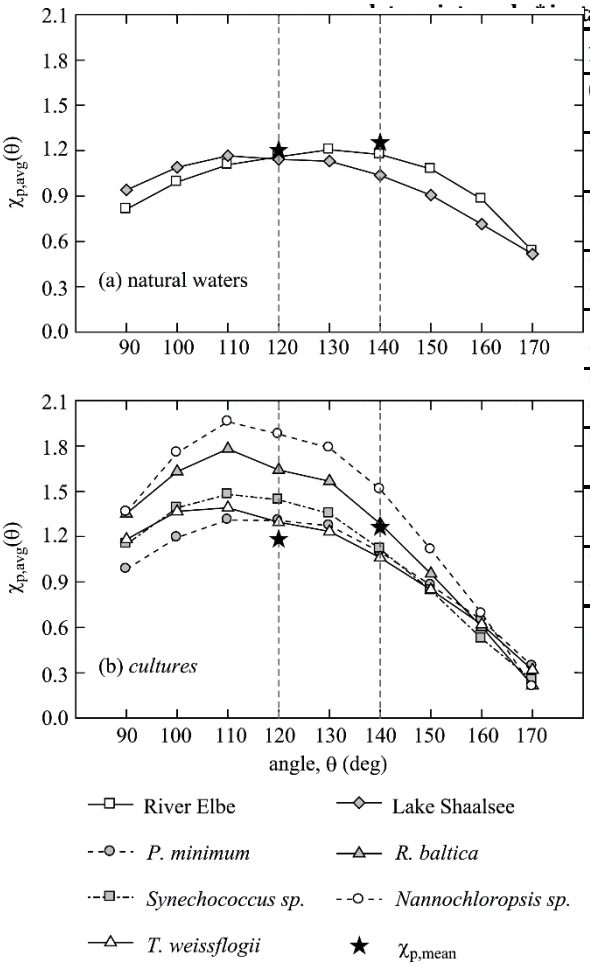


where $\varphi_p(\theta,\lambda)$ is the scaling factor, which connects between $\beta_p(\theta,\lambda)$ and $b_{bp}(\lambda)$ defined as:

$$\varphi_p(\theta,\lambda) = \left[2\pi P_p(\theta,\lambda)\right]^{-1}. \quad \textbf{(5)}$$

In order to develop a practical instrument based on Eq. (4), $\varphi_p(\theta,\lambda)$ should be acceptably constant or predictable by water type and wavelength. Maffione and Dana (1997) thoroughly studied this problem [4], and introduced the alternative parameter, which holds following assumption:

$$\chi_p(\theta) \approx \varphi_p(\theta,\lambda), \quad \textbf{(6)}$$

for all wavelengths, and

$$\chi_p(\theta) \approx \left[2\pi P_p(\theta,\lambda)\right]^{-1}, \quad \textbf{(7)}$$

where $\chi_p(\theta)$ is a wavelength independent conversion factor from $\beta_p(\theta,\lambda)$ to $b_{bp}(\lambda)$ in the same manner as Eq. (5). Then, Eq. (4) can be rewritten using $\chi_p(\theta)$:

$$b_{bp}(\lambda) = 2\pi\chi_p(\theta)\beta_p(\theta,\lambda). \quad \textbf{(8)}$$

Equation (8) is the fixed-angle approach researchers currently use in the practical situations. According to previous studies, θ at 120˚ or 140˚ have been considered to result in the optimum $\chi_p(\theta)$ [3-12]. The values of $\chi_p(120)$ and $\chi_p(140)$ reported in previous studies (hereafter referred to as $\chi_{p,literature}(\theta)$) are provided in Appendix C; let us express the average of $\chi_{pliterature}(\theta)$ as $\chi_{p,mean}(\theta)$. The angular variation of $\chi_{p,avg}(\theta)$, $\chi_p(\theta)$ averaged over measured wavelengths, for the natural waters and cultures that we measured are shown in Fig. 2, compared with $\chi_{p,mean}(\theta)$ at 120˚ and 140˚. Furthermore, our mean values and σ* of $\chi_p(\theta)$ for different backward angles are provided in Table 1.

$\chi_{p,avg}(\theta)$ from 90˚ to 150˚ for natural waters vary less than those for cultures, i.e., σ*<10% for natural waters (see Fig. 2a and Table 1). Recently, Zhang *et al.* (2014) [8] showed that the minimum variability of $\chi_{p,avg}$ occurs at a scattering angle of around 120˚ for VSFs measured from coastal waters with distinct groups of larger particles; their measured values, e.g., $\chi_{p,avg}(122)$=1.19±1.7% (see Fig. 3 in their study), is consistent with $\chi_{p,mean}(120)$ of 1.18. The lowest variation of $\chi_{p,avg}$ for our VSFs for natural waters is found at 124˚, $\chi_{p,avg}(124)$=1.20±3.1%. Furthermore, our $\chi_{p,avg}(122)$ is 1.15±3.6%, which is indeed consistent with $\chi_{p,avg}(122)$ reported by Zhang *et al.* (2014) [8]. The intersection of $\chi_{p,avg}(\theta)$ of River Elbe and Lake Shalsee is at 118˚. $\chi_{p,avg}(120)$ over all natural waters measured is 1.15±4.3%, which is 2.5% less than $\chi_{p,mean}(120)$. River Elbe gave $\chi_{p,avg}(140)$=1.17±2.5%, close to $\chi_{p,literature}(140)$ observed by Boss and Pegau (2001) [5], Sullivan and Twardowski (2009) [6], and Berthon *et al.* (2007) [7]. $\chi_{p,avg}(140)$ for Lake Shaalsee is about 11% less to that of River Elbe, i.e., 1.04±2.6%. Finally, the mean value of our measured natural water $\chi_{p,avg}(140)$ is 1.11±6.8%, 11% less than $\chi_{p,mean}(140)$.

Large variations of $\chi_{p,avg}(\theta)$ from 90˚ to 150˚ are found for cultures (see Fig. 2b and Table 1). In particular, $\chi_{p,avg}(\theta)$ values near 120˚ are highly dependent on types of phytoplankton cultures; $\chi_{p,avg}(120)$ range from 1.30 (*P. minimum* and *T. weissflogii*) to 1.88 (*Nannochloropsis sp.*). $\chi_{p,avg}(120)$ for all cultures are about ~68% higher than $\chi_{p,mean}(120)$. $\chi_{p,avg}(140)$ values of different cultures are vary significantly around $\chi_{p,mean}(140)$, e.g., 15% less than $\chi_{p,mean}(40)$ for *T. weissflogii*, and 21% more for *Nannochloropsis sp.*.

Figure 3 presents the spectral variation of $\chi_{p,avg}(\theta)$ over measured wavelengths at selected angles of 120˚ and 140˚ for natural waters and for cultures. $\chi_{p,mean}(\theta)$ at 120˚ and 140˚ are also shown in the figures as references. $\chi_{p,avg}(120)$ for River Elbe and Lake Shaalsee increase slightly with wavelength, as shown in Fig. 3a; on average, $\chi_{p,avg}(120)$ at 700 nm is about 12% higher than at 400 nm. The maximum difference between $\chi_{p,avg}(120)$ of the natural waters and $\chi_{p,mean}(120)$ is -12% at 400 nm. In regard to $\chi_{p,avg}(140)$, we find small spectral dependencies between both River Elbe and Lake Shaalsee. The deviations of the River Elbe and Lake Shaalsee $\chi_{p,avg}(140)$ are on average 6% and 17% less than $\chi_{p,mean}(140)$, respectively (see Fig. 3c). Thus, Eq. (6) and Eq. (8) are acceptable first approximations for scattering of visible wavelengths at angles of 120˚ and 140˚ in natural waters.

Significant spectral variations of $\chi_{p,avg}(\theta)$ are evident at both 120˚ and 140˚, in the case of phytoplankton cultures (see Fig. 3b and 3d).

$\chi_{p,avg}(120)$ for cultures tend to be higher than $\chi_{p,mean}(120)$, increasingly so towards the red part of the spectrum. The maximum difference between $\chi_{p,avg}(120)$ for any culture and $\chi_{p,mean}(120)$ is +110% at 700 nm for *Nannochloropsis sp.*. Furthermore, the strength of wavelength dependency varies greatly by species of cultures. $\chi_{p,avg}(140)$ also tend to increase with wavelength for cultures, but moderately, compared with $\chi_{p,avg}(120)$.

It is also interesting to note that $\chi_{p,avg}(\theta)$ at both 120° and 140° for cultures of phytoplankton decrease around 480 nm and 680 nm, the strong absorption bands of chlorophyll-a, which is contained in phytoplankton. These results indicate that the spectral shape of $\chi_{p,avg}(\theta)$ is highly dependent on algae species, in agreement with conclusions made by Chami *et al.* (2006) [10]. The magnitude of $\chi_{p,avg}(\theta)$ in algal cultures is a function of wavelength, implying limited

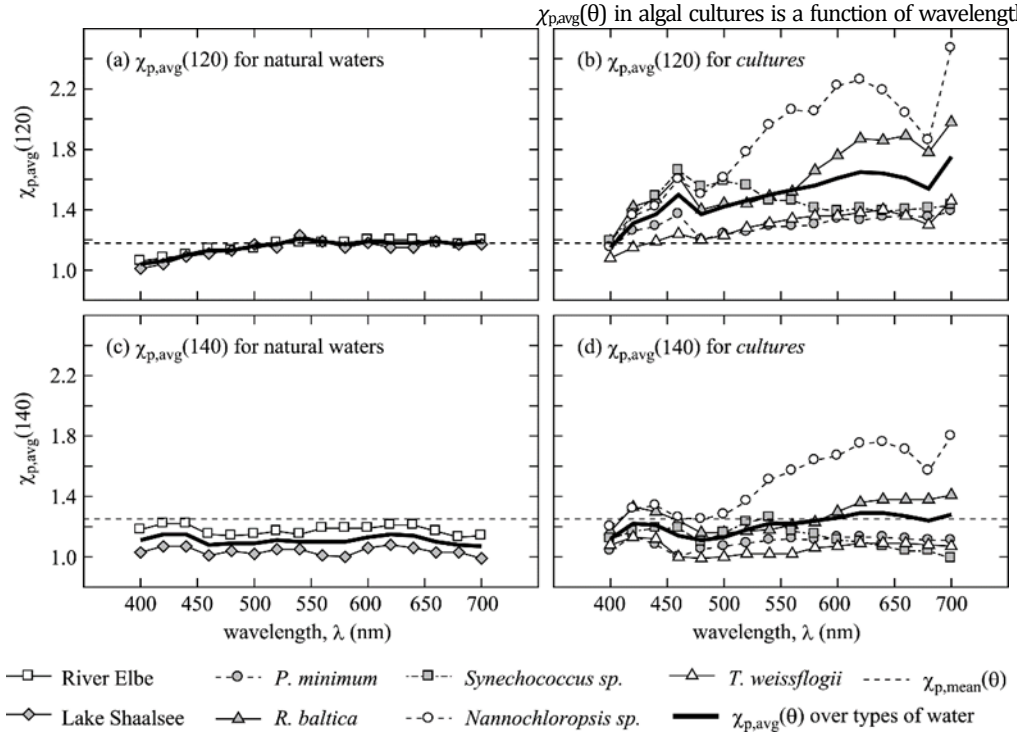


Fig. 3. Wavelength variation of $\chi_{p,avg}(\theta)$ at 120° and 140° for natural waters and cultures of phytoplankton; (a,b) $\chi_{p,avg}(120)$, and (c,d) $\chi_{p,avg}(140)$, respectively. The bold lines are the average of $\chi_p$ over types of water measured. Note that, $\chi_{p,avg}(\theta)$ for cultures are calculated including all concentrations. The horizontal dashed line is shown at $\chi_{p,mean}$ at 120° and 140°, respectively (see Appendix C).

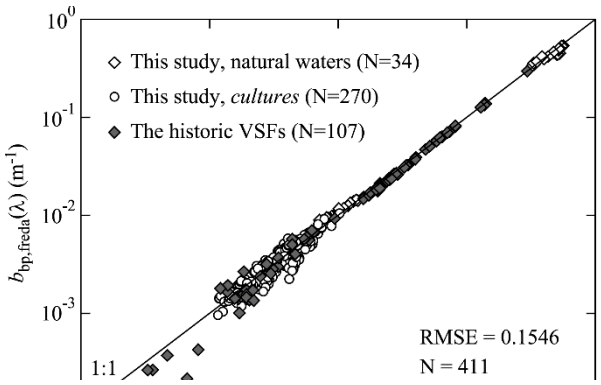


Fig. 4. Comparison of $b_{bp,freda}(\lambda)$ with $b_{bp,integral}(\lambda)$ for VSFs reported here and in previous studies [7-12].

applicability of Eq. (6) and Eq. (8).

Recently, based on VSFs observations in the southern Baltic Sea, Freda (2012) [12] found that $\varphi_p(140,\lambda)$ increases linearly with wavelength ($r^2$>0.99). Using our measured VSFs as well as tabulated VSFs in the literature [17-21], we verify this relation; we compare $b_{bp,Freda}$, $b_{bp}(\lambda)$ estimated using $\varphi_p(140,\lambda)$ derived from this relation in Eq. (4), with $b_{bp,integral}$, $b_{bp}(\lambda)$ directly determined using Eq. (2). The maximum difference between $b_{bp,Freda}(\lambda)$ and $b_{bp,integral}(\lambda)$ is 68% for natural waters, including literature values, and 50% for cultures (see Fig. 4). The average prediction error between $b_{bp,Freda}$ and $b_{bp,integral}$ is approximately 12%, with only 22% of data points falling within ±5% of the estimation error, i.e., 0.1546 of the root mean square error (RMSE). This result suggests us that Freda's relation is not accurate when applied to different types of waters than those in his study.

From the analysis of measured $\beta_p(\theta,\lambda)$ and $\chi_p(\theta)$ presented in this section, values and trends of $\chi_p(\theta)$ at 120° and 140° agree with those found in the literature, and we reach several conclusions. First, the assumption of Eq. (6) does not hold for all types of waters. Therefore, Eq. (8) is a first approximation to be made with caution. Second, it is difficult to express the spectral variation of $\varphi_p(\theta,\lambda)$ in a simple form, applicable to all types of waters, in agreement with Chami *et al.* (2006) [10] and Freda (2012) [12]. Finally, Eq. (4) and Eq. (8) are unlikely to result in more accurate estimates of $b_{bp}(\lambda)$.

In the next section, we will propose an alternative conversion factor that is independent of water types and wavelengths, thus overcoming the problems mentioned above.

## 4. Universal conversion factor for particulate backscattering and improved fixed-angle approach

We first revisit the analysis of VSF measurements in more detail, and introduce the following function:

$$Q_p(\theta,\lambda)=\frac{2\pi\int_{\theta}^{\theta+\Delta\theta}\beta_p(\theta,\lambda)\sin\theta d\theta}{b_{bp}(\lambda)}, \qquad \textbf{(9)}$$

where θ goes from 90° to 180°. $Q_p(\theta,\lambda)$ gives the fractional contribution of the scattering by particles within Δθ (0.5°, in this study) of a given θ to $b_{bp}(\lambda)$. Figure 5 presents $Q_{p,avg}(\theta)$, average of $Q_p(\theta,\lambda)$ over measured λ, in ascending order of $\varphi_{p,avg}(120)$, average of $\varphi_p(\theta,\lambda)$ over measured λ, of which values and σ* are shown at top of the figures, respectively.

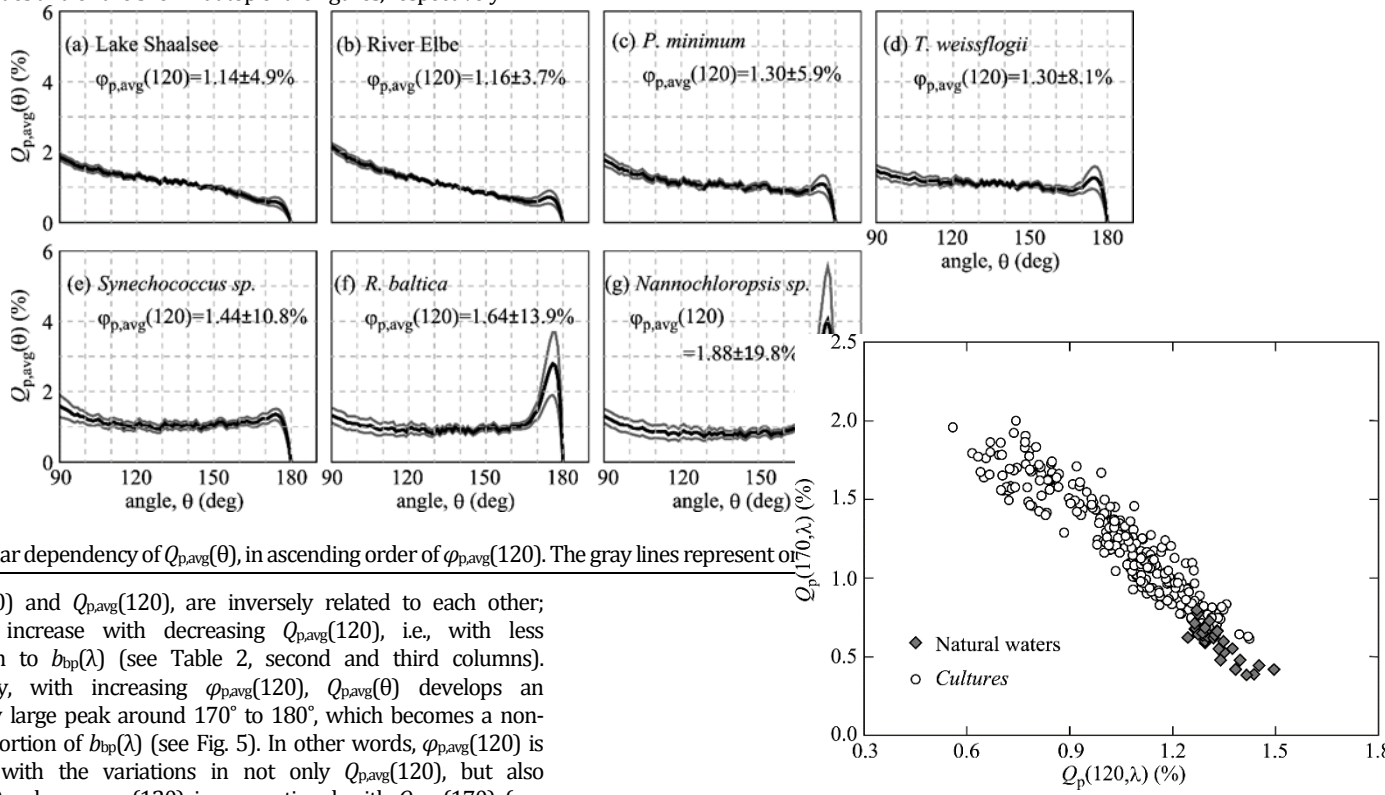


Fig. 5. Angular dependency of $Q_{p,avg}(\theta)$, in ascending order of $\varphi_{p,avg}(120)$. The gray lines represent or

$\varphi_{p,avg}(120)$ and $Q_{p,avg}(120)$, are inversely related to each other; $\varphi_{p,avg}(120)$ increase with decreasing $Q_{p,avg}(120)$, i.e., with less contribution to $b_{bp}(\lambda)$ (see Table 2, second and third columns). Interestingly, with increasing $\varphi_{p,avg}(120)$, $Q_{p,avg}(\theta)$ develops an increasingly large peak around 170° to 180°, which becomes a non-negligible portion of $b_{bp}(\lambda)$ (see Fig. 5). In other words, $\varphi_{p,avg}(120)$ is associated with the variations in not only $Q_{p,avg}(120)$, but also $Q_{p,avg}(170\sim)$, where $\varphi_{p,avg}(120)$ is proportional with $Q_{p,avg}(170)$ (see Table 2, second and fourth columns). We can therefore say that $Q_p(120,\lambda)$ covaries with $Q_p(170,\lambda)$ roughly inversely, as shown in Fig. 6. These results suggest the influence of backscattering for θ>170° should be accounted for to obtain a more accurate conversion factor. A natural metric to account for this high-angle backscattering and quantify shape variations in VSFs is the ratio of $Q_p(\theta_1,\lambda)$ to $Q_p(\theta_2,\lambda)$, $R_p^*(\theta_1,\theta_2)=Q_p(\theta_2,\lambda)/Q_p(\theta_1,\lambda)$, where $\theta_1$=120° and $\theta_2$=170°. However, it is not practical to use $R_p^*(\theta_1,\theta_2)$. Noting that $\beta_p(\theta,\lambda)$ is a moderate function of θ in the backward direction and Δθ is infinitesimal, $R_p^*(\theta_1,\theta_2)$ can be approximated as:

$$\begin{aligned}
R_p^*(\theta_1,\theta_2)&=\frac{Q_p(\theta_2,\lambda)}{Q_p(\theta_1,\lambda)}\\
&=\frac{\int_{\theta_2}^{\theta_2+\Delta\theta}\beta_p(\theta_2,\lambda)\sin\theta}{\int_{\theta_1}^{\theta_1+\Delta\theta}\beta_p(\theta_1,\lambda)\sin\theta}.\\
&\approx\frac{\frac{1}{2}\left[\beta_p(\theta_2,\lambda)+\beta_p(\theta_2+\Delta\theta,\lambda)\right]\sin\left(\theta_2+\frac{\Delta\theta}{2}\right)\Delta\theta}{\frac{1}{2}\left[\beta_p(\theta_1,\lambda)+\beta_p(\theta_1+\Delta\theta,\lambda)\right]\sin\left(\theta_1+\frac{\Delta\theta}{2}\right)\Delta\theta}\\
&=A\frac{\beta_p(\theta_2,\lambda)+\beta_p(\theta_2+\Delta\theta,\lambda)}{\beta_p(\theta_1,\lambda)+\beta_p(\theta_1+\Delta\theta,\lambda)}\\
&=A\left[\begin{array}{l}\dfrac{\beta_p(\theta_2,\lambda)}{\beta_p(\theta_1,\lambda)}\dfrac{1}{\left(1+\dfrac{\beta_p(\theta_1+\Delta\theta,\lambda)}{\beta_p(\theta_1,\lambda)}\right)}\\ +\dfrac{\beta_p(\theta_2+\Delta\theta,\lambda)}{\beta_p(\theta_1,\lambda)}\dfrac{1}{\left(1+\dfrac{\beta_p(\theta_1+\Delta\theta,\lambda)}{\beta_p(\theta_1,\lambda)}\right)}\end{array}\right],
\end{aligned} \qquad \textbf{(10)}$$

where $A$ is a proportionality constant. For sufficiently small $\Delta\theta$, $\beta_p(\theta_1+\Delta\theta,\lambda)/\beta_p(\theta_1,\lambda)\approx 1$, and $\beta_p(\theta_2+\Delta\theta,\lambda)/\beta_p(\theta_1,\lambda)\approx\beta_p(\theta_2,\lambda)/\beta_p(\theta_1,\lambda)$. We can thus further simplify the approximation of $R_p^*(\theta_1,\theta_2)$ as:

$$R_p^*(\theta_1,\theta_2) \approx A\left[\frac{1}{2}\frac{\beta_p(\theta_2,\lambda)}{\beta_p(\theta_1,\lambda)}+\frac{1}{2}\frac{\beta_p(\theta_2,\lambda)}{\beta_p(\theta_1,\lambda)}\right] = A\frac{\beta_p(\theta_2,\lambda)}{\beta_p(\theta_1,\lambda)}. \quad (11)$$

We define $R_p(\theta_1,\theta_2)$ to eliminate $A$ and indicate the shape of VSF for backward angles using $\beta_p(\theta,\lambda)$ as:

$$R_p(\theta_1,\theta_2) = \frac{1}{A}R_p^*(\theta_1,\theta_2) = \frac{\beta_p(\theta_2,\lambda)}{\beta_p(\theta_1,\lambda)}. \quad (12)$$

Consequently, in the case of $\theta_1=120^\circ$ and $\theta_2=170^\circ$, we have $R_p(120,170)=\beta_p(170,\lambda)/\beta_p(120,\lambda)$.

Figure 7 shows the relation between $\varphi_p(120,\lambda)$ determined by Eq. (5) and $R_p(120,170)$. The relationship between them is well fit by an exponential function (N=304, $r^2$>0.96). In other words, we can accurately estimate $\varphi_p(120,\lambda)$ from $\beta_p(120)$ and $\beta_p(170)$ as:

$$\varphi_p(120,\lambda) = 0.9939e^{0.0636R_p(120,170)} \quad (r^2=0.96). \quad (13)$$

Wavelength affects $R_p(120,170)$, since it affects the parameterized shape of $\beta_p(\theta,\lambda)$. To avoid confusion, $\varphi_p(120,\lambda)$ estimated from empirical regression of Eq. (13) is hereafter denoted:

$$\nu_p\left[R_p(120,170)\right] \equiv \varphi_p(120,\lambda), \quad (14)$$

where $\nu_p[R_p(120,170)]$ is the universal particulate conversion factor for $b_{bp}(\lambda)$. As a consequence, the rigorous fixed-angle approach (Eq. 4) can be reformulated using $\nu_p[R_p(120,170)]$:

$$b_{bp}(\lambda) = 2\pi\nu_p\left[R_p(120,170)\right]\beta_p(120,\lambda). \quad (15)$$

For readers' convenience, coefficients of the exponential function for different scattering angle combinations are presented in Appendix D.

Fig. 6. Interrelationship between $Q_p(120,\lambda)$ and $Q_p(170,\lambda)$.

**Table 3. Summary of quantified errors in the fixed-angle approach by the use of different conversion factors for $\beta_p(\theta,\lambda)$ based on the Lorenz-Mie calculations.**

| Types of waters | N | | Conversion factor used for $b_{bp}(\lambda)$ estimation | |
|---|---|---|---|---|
| | | | $\nu_p[R_p(120,170)]$ | $\chi_{p,mean}(120)$ |
| Junge PSD | 450 | RMSE | 0.0331 | 0.0989 |
| | | Average of $\lvert\Delta b_{bp,\nu p}\rvert$ or $\lvert\Delta b_{bp,\chi p}\rvert$ | 1.9 % | 9.5 % |
| | | Frequency within ±5% of $\Delta b_{bp,\nu p}$ or $\Delta b_{bp,\chi p}$ | 92 % | 6 % |
| Gauss PSD | 972 | RMSE | 0.1338 | 0.1290 |
| | | Average of $\lvert\Delta b_{bp,\nu p}\rvert$ or $\lvert\Delta b_{bp,\chi p}\rvert$ | 9.6 % | 9.3 % |
| | | Frequency within ±5% of $\Delta b_{bp,\nu p}$ or $\Delta b_{bp,\chi p}$ | 43 % | 23 % |

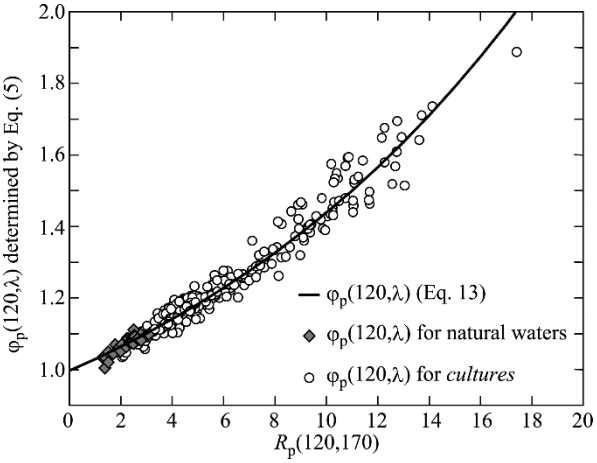


Fig. 7. Relationship between $R_p(120,170)$ and $\varphi_p(120,\lambda)$ determined by Eq. (5), for natural waters and cultures of phytoplankton measured (N=304). The bold line shows the empirical function of $\varphi_p(120,\lambda)$ (Eq. 13, $r^2$=0.96), i.e., $\nu_p[R_p(120,170)]$.

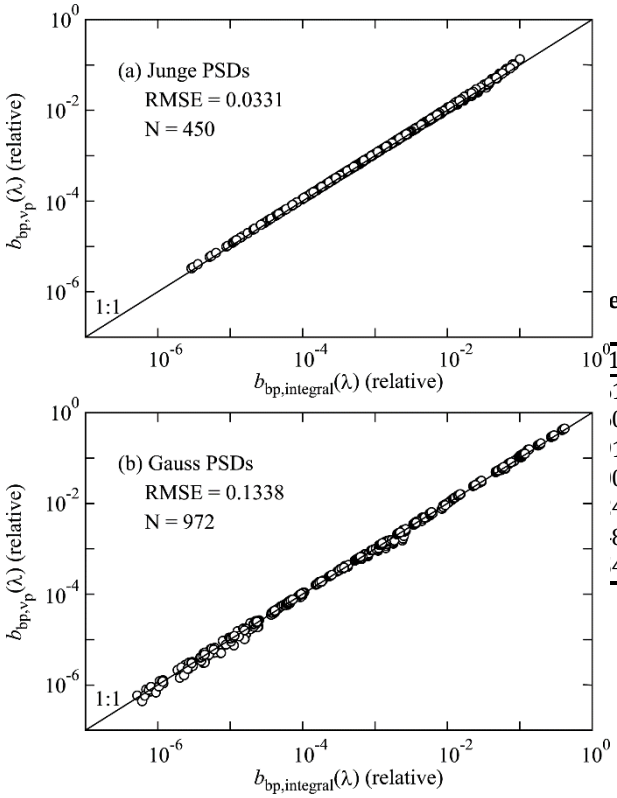


Other angle combinations can be used to make accurate estimates of $b_{bp}(\lambda)$; for instance, $\theta_1=117^\circ$ and $\theta_2=170^\circ$, $\theta_1=118^\circ$ and $\theta_2=170^\circ$, or $\theta_1=119^\circ$ and $\theta_2=170^\circ$. Since most previous studies have focused on the relation between $\beta_p(120,\lambda)$ and $b_{bp}(\lambda)$ [3-12], we evaluate the proposed fixed-angle approach with the angle combination of $\theta_1=120^\circ$ and $\theta_2=170^\circ$, hereafter. Note that the empirical relation of Eq. (13) is obtained based on only VSF datasets measured in this study.

## 5. Evaluation of proposed fixed-angle approach

### A. Lorenz-Mie scattering

Lorenz-Mie scattering is a useful first approximation of scattering behavior in the sea, although it assumes spherical particles [22]. Lorenz-Mie theory is thus can be used to verify whether our proposed fixed-angle approach accurately estimates $b_{bp}(\lambda)$. We made calculations assuming various particle size distributions (PSDs) and a complex refractive index relative to water, $m=n-i\kappa$. In this study, we assume PSD to follow either (1) a hyperbolic law (Junge distribution) to model natural waters, or (2) a Gaussian distribution to model phytoplankton blooms [3, 23]. Incident wavelengths of 400 nm, 550 nm, and 700 nm are considered for both PSDs. The covariance of the real and imaginary parts of the complex refractive index as a function of wavelength, i.e., the anomalous dispersion of the refractive index, is not considered. In total, we computed 1422 Lorenz-Mie VSFs; N=450 Junge PSDs and N=972 Gauss PSDs.

Junge PSDs take the form $N(D)\sim D^{\xi}$, where $N(D)$ is the number of particles larger than a given particle diameter, $D$ (μm), and $\xi$ is the Junge exponent. $D$ ranges from 0.01 μm to 100.0 μm and $\xi$ ranges from 2.8 to 4.4 in this study [23, 24]. Note that $N(D)$ is normalized by the total number of particles. The effective real part of the refractive index, $n$, varies from 1.02, representative of biogenic particles (phytoplankton), to 1.20, representative of minerogenic particles [25,26], by increments of 0.02. The imaginary part, $\kappa$, is 0.000, 0.005, or 0.010 [27]. For Gauss PSDs, geometric mean diameters are varied from 0.05 μm to 100.0 μm under the same number of particles as the Junge PSD simulations, i.e., $\pm 3\sigma$, $n$ ranges from 1.02 to 1.06 in 0.01 increments [25], and $\kappa$ is 0.000, 0.005, or 0.010.

We start by briefly confirming the results of our Lorenz-Mie calculations by comparing with previous results; Oishi (1990) showed that $\chi_{p,avg}(120)$ based on his Lorenz-Mie VSFs is 1.10±6% for natural waters, and 1.15±24% for phytoplankton bloom waters, respectively [3]. Lorenz-Mie VSFs from our computations give $\chi_{p,avg}(120)$ of 1.08±3% for natural waters, and 1.18±18% for phytoplankton blooms, which are consistent with the values reported by Oishi (1990) [3].

We present the correlation between $b_{bp,vp}$ and $b_{bp,integral}$ for both PSDs in Fig. 8, and the performance of the fixed-angle approaches using $\nu_p[R_p(120,170)]$ as well as $\chi_{p,mean}(120)=1.18$ applied to as Lorenz-Mie VSFs are also shown in Table 3. Our fixed-angle approach for Junge PSD estimates $b_{bp}(\lambda)$ better than the conventional method; $b_{bp,vp}$ and $b_{bp,\chi p}$ had mean estimation errors of 1.9% and 9.5% and RMSEs of 0.0331 and 0.0989, respectively. Surprisingly, 92% of data points fell within ±5% of $\Delta b_{bp,vp}$. By contrast, our fixed-angle approach for Gauss PSDs and the conventional method of estimating $b_{bp}(\lambda)$ (Eq. 15 and Eq. 8) gave similar quantitative errors, for all cases considered (see Table 3); both gave roughly 9.5% of the mean estimation error and 0.13 of RMSE. An obvious difference appeared in the frequency of data points within ±5% of the prediction error. Our approach increased that percentage by a factor of two compared with the conventional approach, i.e., 43% from 23%. Based on Fig. 8 and Table 3, we found that our proposed approach can improve the $b_{bp}(\lambda)$ estimation accuracy, or at least match, the capability of the classical approach, indicating the reliability of Eqs. (13) to (15).

**Table 4. Summary of quantified errors in the fixed-angle approach by the use of different conversion factors for measured $\beta_p(\theta,\lambda)$ .**

| Types of waters | N | | Conversion factor used for $b_{bp}(\lambda)$ estimation | |
|---|---|---|---|---|
| | | | $\nu_p[R_p(120,170)]$ | $\chi_{p,mean}(120)$ |
| Natural waters with the historic VSFs | 141 | RMSE | 0.0472 | 0.0800 |
| | | Average of $\lvert\Delta b_{bp,vp}\rvert$ or $\lvert\Delta b_{bp,\chi p}\rvert$ | 3.4 % | 6.1 % |
| | | | | 55 % |
| *Cultures* | | | | 0.2384 |
| | | | | 19.7 % |
| | | | | 13 % |

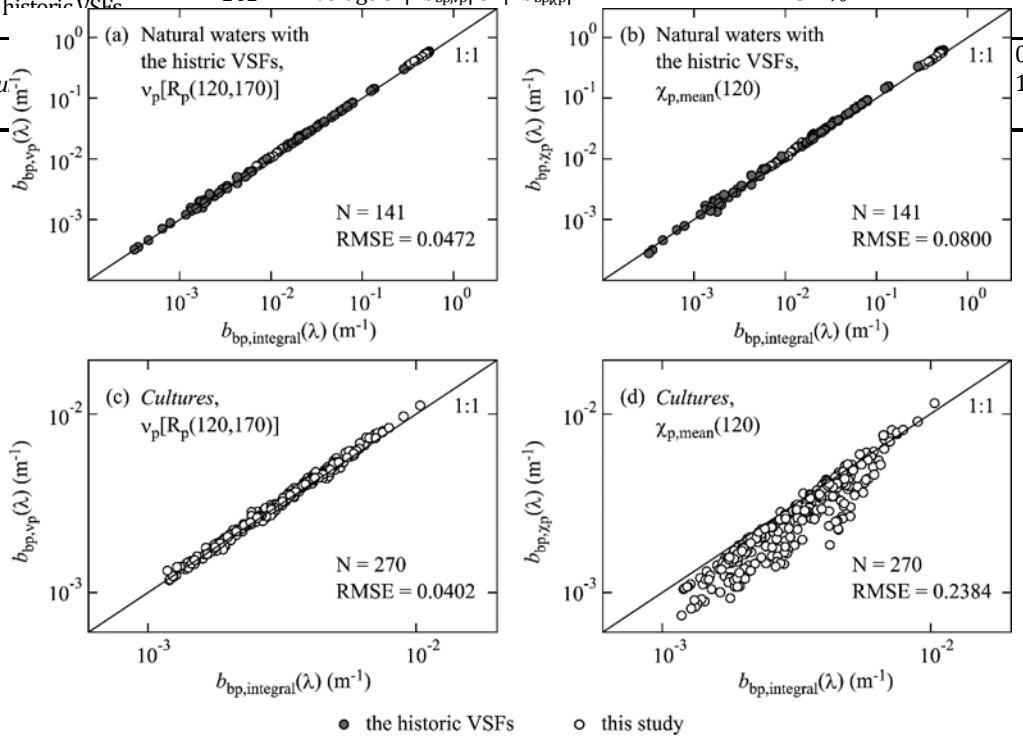


Fig. 9. Performance of the estimate of $b_{bp}(\lambda)$ with the fixed-angle approach by the use of either $\nu_p[R_p(120,170)]$ or $\chi_{p,mean}(120)$ as 1.18. $b_{bp,vp\ or\ \chi p}(\lambda)$ against $b_{bp,integral}(\lambda)$; for natural waters including the historic VSFs dataset with (a) $\nu_p[R_p(120,170)]$, (b) $\chi_{p,mean}(120)$, and for cultures of phytoplankton with (c) $\nu_p[R_p(120,170)]$, (d) $\chi_{p,mean}(120)$, respectively.

**B. Measured VSFs**

In Fig. 9, we present the results of comparisons between $b_{bp,\nu p}$, $b_{bp,\chi p}$ and $b_{bp,integral}$ VSFs measured for different types of oceanic waters over all wavelengths. Quantified errors from the fixed-angle approach using $\nu_p[R_p(120,170)]$ and $\chi_{p,mean}(120)$ are provided in the third and fourth columns of Table 4. We evaluated 411 VSF datasets, including VSFs measured here (N=304) and VSFs from the literature (N=107) [17-21]. The first column in Appendix E gives background information about the historic VSFs, including observer, location, and λ. of the VSF measurement. For reference, $\chi_{p,avg}(120)$ and $\nu_{p,avg}[R_p(120,170)]$, average of $\nu_p[R_p(\theta_1,\theta_2)]$, for the historic VSFs used in the evaluation are given in the third and fourth column, and the percent deviations between them are in the fifth column of Appendix E as well. To obtain $b_{bp}(\lambda)$, $\beta_p(\theta,\lambda)$ from the literature are linearly extrapolated on a log-scale. Note that the magnitude of $\beta_p(\theta,\lambda)$ for Lee *et al.* (2003) [19] and Mankovsky and Haltrin (2002) [20, 21] are determined by iterating calculations until the total scattering coefficient is sufficiently close (within ±1%) to that stated in the literature, since they are given as phase functions. We excluded data for which $\beta_p(\theta)$ becomes negative after subtraction of scattering by pure seawater.

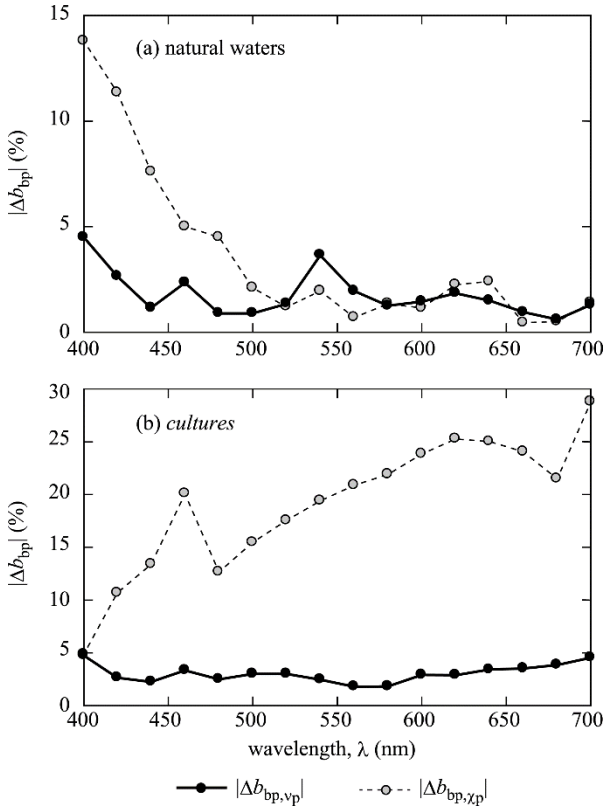


Fig. 10. $|\Delta b_{bp,\nu p}|$ and $|\Delta b_{bp,\chi p}|$ as functions of wavelength from VSFs measured: (a) natural waters, (b) cultures of phytoplankton.

Using $\nu_p[R_p(120,170)]$ significantly improves the accuracy of estimates of $b_{bp}(\lambda)$ over a large dynamic range for VSFs measured in natural waters, even for the VSFs in the literature (see Fig. 9a); $|\Delta b_{bp,\nu p}|$'s are as low error as 3.4% on average (0.0472 RMSE), and about 76% of data points fall within ±5% $\Delta b_{bp,\nu p}$ error. On the other hand, the mean $|\Delta b_{bp,\chi p}|$ is 6.1%, approximately two times as large as that of $|\Delta b_{bp,\nu p}|$ (see Fig. 9b) for VSFs of natural waters, including literature values. Around 55% of data points are within ±5% $\Delta b_{bp,\chi p}$ error, which results in 0.0800 RMSE. Our approach becomes remarkably significant for cultures of phytoplankton (see Fig. 9c). Specifically, the overall $|\Delta b_{bp,\nu p}|$ is as small as 3.2% (0.0402 RMSE), and more than 80% of the data points fall within ±5% $\Delta b_{bp,\nu p}$ error. By contrast, the estimates of $b_{bp}(\lambda)$ with $\chi_{p,mean}(120)$ lead to 19.7% $|\Delta b_{bp,\chi p}|$ on average (0.2384 RMSE), as shown in Fig. 9d. Only 13% of data points are within ±5% $\Delta b_{bp,\chi p}$ error. This result indicates that the proposed method accurately estimates $b_{bp}(\lambda)$ for phytoplankton rich or blooming waters, with almost the same accuracy as for natural waters.

The function of $\nu_p[R_p(120,170)]$ is derived by taking into account the shape of $\beta_p(\theta,\lambda)$ in backward directions, which depends on water types and wavelengths. As a result, we can improve the accuracy of the estimation of $b_{bp}(\lambda)$ in the visible spectrum by using $\nu_p[R_p(120,170)]$ (see $|\Delta b_{bp,\nu p}(\lambda)|$ in Fig. 10). In contrast, $|\Delta b_{bp,\chi p}|$ significantly varies as a function of wavelength: $|\Delta b_{bp,\chi p}(\lambda)|$ tends to decrease towards red wavelengths in natural waters, and has a maximum of 14% at 400 nm (see Fig. 10a). For cultures of phytoplankton, $|\Delta b_{bp,\chi p}(\lambda)|$ increases with λ, reaching a maximum difference of 29% at 700 nm (see Fig. 10b). Based on VSF observations, Chami *et al.* (1996) [10] revealed that a fixed-angle approach with constant $\chi_p(140)$ for the discrete visible spectrum results in a mean $b_{bp}(\lambda)$ estimation error of 7% for natural waters and 26% for algal cultures. These values are consistent with our measurements using $\chi_{p,mean}(120)$, as shown in Table 4. Hence, we conclude that the use of a constant $\chi_p(120)$ in the fixed-angle approach (Eq. 8) induces significant error in the estimate of $b_{bp}(\lambda)$, especially for phytoplankton rich waters, in agreement with conclusions made by

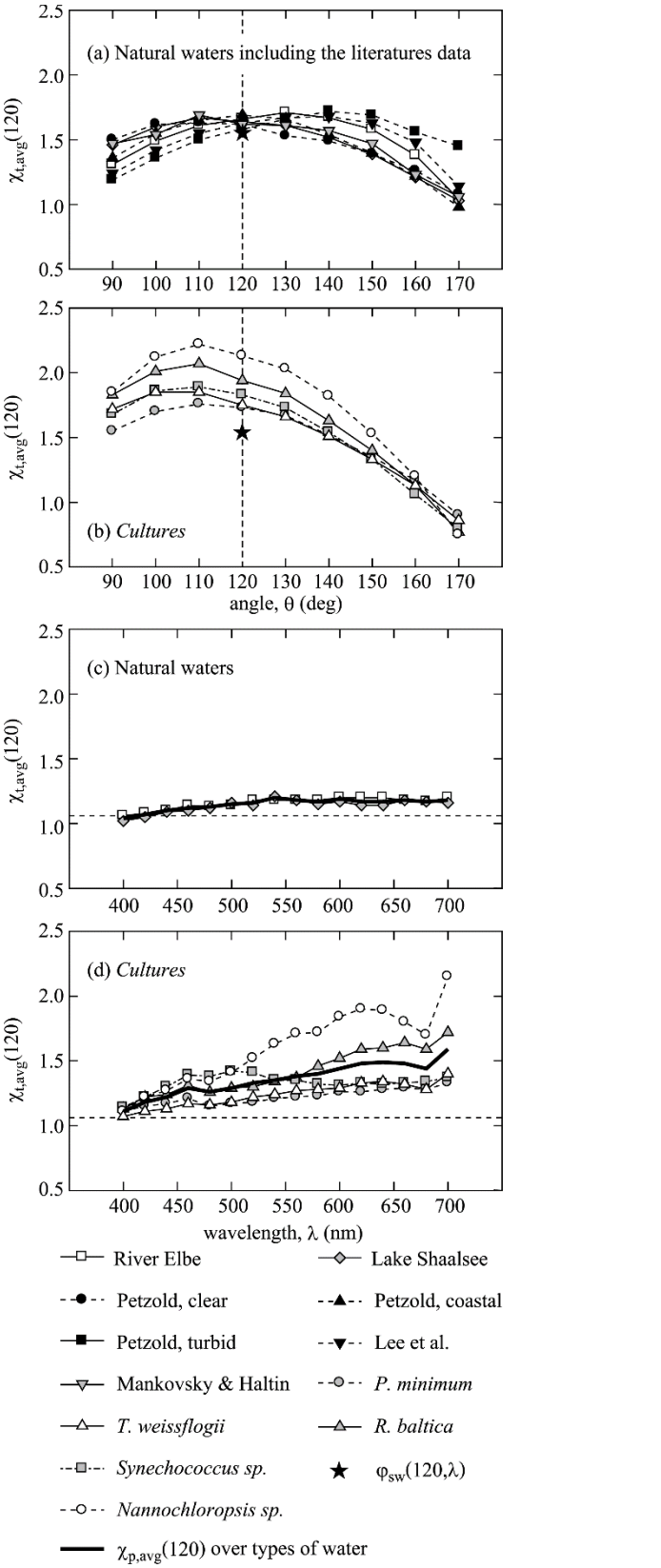


Chami *et al.* (2006) [10]. From our measurements, the variability of $\chi_p(120)$ depends on water types and wavelengths, especially in

Fig. 11. $\chi_{t,avg}(120)$ dependence on scattering angle and wavelength. Angular variation of $\chi_{t,avg}(120)$ for (a) natural waters including literature data, and (b) cultures of phytoplankton averaged over all concentrations. The 'star" symbol in (a) and (b) shows $\varphi_{sw}(120,\lambda)=1.06$. Wavelength variation of $\chi_{t,avg}(120)$ for (c) natural waters, and (d) cultures of phytoplankton. The horizontal dashed lines in (c) and (d) show $\varphi_{sw}(120,\lambda)$. The bold lines are the average of $\chi_t(120)$ over types of water measured in this study.

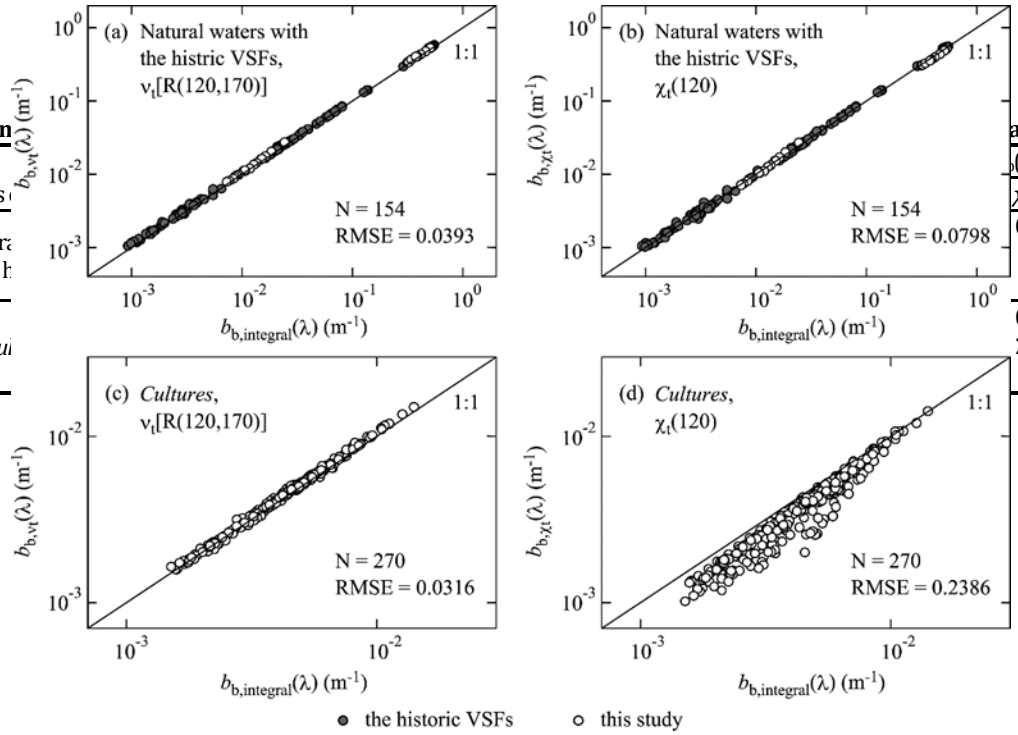


Fig. 12. Comparison between $b_{b,\nu t\ or\ \chi t}(\lambda)$ and $b_{bp,integral}(\lambda)$ for our natural waters with the historic VSFs using (a) $\nu_t[R(120,170)]$, (b) $\chi_t(120)$ =1.06, and for phytoplankton cultures using (c) $\nu_t[R(120,170)]$, (d) $\chi_t(120)$=1.06, respectively.

cultures of microalgal phytoplankton, for which the spectral shape is currently unpredictable. Furthermore, we found large variations in $\chi_p(\theta)$ for cultures, in the vicinity of 480 nm and 680 nm, the strong absorption wavelengths of chlorophyll-a (see Fig. 3b and 3d). This is probably due to the influence of absorption on scattering via anomalous dispersion of the refractive index [10,28,29], which alters the shape of VSF in backward direction. Thus, it should be possible to attain a generalized expression of $\varphi_p(\theta,\lambda)$ by examining the relationship between absorption and VSF, in detail. On account of the universal conversion factor $\nu_p$, however, the fixed-angle approach introduced in this study can provide reliable estimates of $b_{bp}(\lambda)$ for all types of water, with <3% of the mean error. Our approach can be universally applied, easily adaptable to natural waters, as well as phytoplankton rich or bloom waters.

## 6. Universal conversion factor for total scattering coefficient and improved fixed-angle approach

The rigorous fixed-angle approach for $b_b(\lambda)$ is defined as:

$$b_b(\lambda) = 2\pi\varphi_t(\theta,\lambda)\beta(\theta,\lambda), \quad \textbf{(16)}$$

where $\varphi_t(\theta,\lambda)$ is the scaling factor of the phase function of the bulk VSF, $P(\theta,\lambda)=\beta(\theta,\lambda)/b_b(\lambda)$. Further,

$$\varphi_t(\theta,\lambda) = \left[2\pi P(\theta,\lambda)\right]^{-1}. \quad \textbf{(17)}$$

Similar to Eq. (6), we assume:

$$\chi_t(\theta) \approx \varphi_t(\theta,\lambda), \quad \textbf{(18)}$$

where $\chi_t(120)$ is the spectrally constant conversion factor, related to $\beta(\theta,\lambda)$ and $b_b(\lambda)$. Therefore, the fixed-angle approach currently used in practice is expressed as:

$$b_b(\lambda) = 2\pi\chi_t(\theta)\beta(\theta,\lambda). \quad \textbf{(19)}$$

Conversion factors, $\chi_t$, $\chi_p$, and $\varphi_{sw}$ for pure seawater are currently assumed to be nearly equal, i.e., $\chi_t(120)\approx\chi_p(120)\approx\varphi_{sw}(120,\lambda)\approx1.06$ [5]. However, our experimental datasets show that this relation does not hold for all types of waters, in particular, for cultures of phytoplankton. The average $\chi_t(120)$ for natural waters, including historical datasets [17,19-21] is 1.13±5.6%, which is a 7% deviation from $\varphi_{sw}(120,\lambda)$=1.06 (see Fig. 11a). As for cultures of phytoplankton, the average $\chi_t(120)$ deviates from 15% (*P. minimum*) to 51% (*Nannochloropsis sp.*), as shown in Fig. 11b. Further, $\chi_t(120)$ is a function not only of water types, but also of wavelength (see Fig. 11c and 11d). These results imply that Eq. (19) is a first approximation. Using $\chi_t(120)=\varphi_{sw}(120,\lambda)=1.06$ in Eq. (19) results in a mean $|\Delta b_{b,\chi t}|$ of 6.9% for natural waters, including the data from the literature [17,19-21] (see Fig. 12b). 34% data points are within ±5% $\Delta b_{b,\chi t}$ error (0.0798 RMSE). As for cultures, the mean $|\Delta b_{b,\chi t}|$ is 21.1% (see Fig. 12d), and only 4% of data points are within ±5% $\Delta b_{b,\chi t}$ error (0.2386 RMSE). Hence, Eq. (19) only applies for natural waters, not for phytoplankton rich or blooms. That is, we should be conservative using $\chi_t(120)$ in practical situations. Deviations from $\varphi_{sw}(\theta,\lambda)$ are due to the magnitudes of $\varphi_t(\theta,\lambda)$, which are associated with the shape of $\beta(\theta,\lambda)$, especially for θ>170°. That is, $Q(120)$, the contribution of the angular backscattering coefficient at 120° to $b_b(\lambda)$, is inversely proportional to $Q(170)$, in the same manner as particle scattering, as shown in Fig. 6. Similar to $\varphi_p(\theta,\lambda)$, therefore, $\varphi_t(\theta,\lambda)$ becomes larger with increasing $\beta(\theta,\lambda)$ for θ>170° (see Table 2, second and fourth columns).

The exponential function of $R(120,170)$, i.e., the VSF ratio $\beta(170,\lambda)/\beta(120,\lambda)$, should be applicable in estimating $b_b(\lambda)$, since our approach relies only on the assumption that the VSF ratio between these angles represents the shape differences of VSFs due to oceanic water types and wavelengths. Similarly to Eq. (13), we can estimate $\varphi_t(120,\lambda)$ from:

$$\varphi_t(120,\lambda) = 0.9743e^{0.0684R(120,170)} \quad (r^2 = 0.96). \quad \textbf{(20)}$$

Note that Eq. (20) is obtained based only on the VSFs measured in this study. Hereafter, as in particulate scattering, we denote $\varphi_t(120,\lambda)$ estimated from empirical regression of Eq. (20) as:

$$\nu_t\left[R(120,170)\right] \equiv \varphi_t(120,\lambda), \quad \textbf{(21)}$$

where $\nu_t[R(120,170)]$ is the universal conversion factor for $b_b(\lambda)$, taking into account the shape of $\beta(\theta,\lambda)$. Indeed, Eq. (20) gives $\nu_t[R(120,170)]=1.08$ for $\beta_{sw}(\theta,\lambda)$, i.e., $R(120,170)=1.50$ [15], which is a 1.8% difference relative to $\varphi_{sw}(120,\lambda)$, determined from Eq. (17) to be 1.06. Consequently, $b_b(\lambda)$ can be estimated with:

$$b_b(\lambda) = 2\pi\nu_t\left[R(120,170)\right]\beta(120,\lambda). \quad \textbf{(22)}$$

The quantitative errors in the fixed-angle approaches for $b_b(\lambda)$ estimated with $\nu_t[R(120,170)]$ and $\chi_t(120)=1.06$ are provided in the fifth and sixth columns of Table 5. The average of $|\Delta b_{b,\nu t}|$ for natural waters, including data from the literature [17,19-21] is 3.1% (see Fig. 12a), and approximately 85% of data points are within ±5% $\Delta b_{b,\nu t}$ error (0.0393 RMSE). For cultures of phytoplankton, the average of $|\Delta b_{b,\nu t}|$ is 2.5% (see Fig. 12c), and the frequency with which data points fall within ±5% error is roughly 90% (0.0316 RMSE). These results indicate that the bulk VSF ratio, $\beta(170,\lambda)/\beta(120,\lambda)$, is an appropriate parameter to estimate $b_b(\lambda)$ for most oceanic waters, including phytoplankton rich waters.

We present the coefficients of exponential functions for different scattering angle combinations in Appendix F, for readers' convenience. $\nu_p[R_p(120, 170)]$ (Eq. 13) and $\nu_t[R(120,170)]$ (Eq. 20) are relatively similar exponential functions (see also appendix D and F). The prediction errors of $b_b(\lambda)$ or $b_{bp}(\lambda)$, using our approach, are almost constant through the range of the coefficients analyzed (see Fig. 9a,c and 12a,c). Consequently, the proposed fixed-angle approach is practical for use in routine measurements.

## 7. Conclusions

We introduced the universal conversion factors, $\nu_p$ and $\nu_t$, to estimate $b_{bp}(\lambda)$ and $b_b(\lambda)$ with the parameterized VSF shape indicator, i.e., $R_p(\theta_1,\theta_2)=\beta_p(\theta_2,\lambda)/\beta_p(\theta_1,\lambda)$ and $R(\theta_1,\theta_2)=\beta(\theta_2,\lambda)/\beta(\theta_1,\lambda)$, respectively. Although the empirical relations, Eq. (13) and Eq. (20), were obtained only from VSF datasets measured in this study, these relations hold for most natural waters, as demonstrated through applications to various VSF datasets measured in previous studies (see Fig. 9 and 12). Our approach enables significant improvement in $b_{bp}(\lambda)$ and $b_b(\lambda)$ estimation accuracy. Specifically, we can accurately determine $b_{bp}(\lambda)$ and $b_b(\lambda)$ with 3% of the mean estimation error, independent of wavelength in the visible spectrum and water types, i.e., phytoplankton rich water or not, making our method very practical for *in situ* measurements.

We analyzed performance using the angle combination of $\theta_1=120^\circ$ and $\theta_2=170^\circ$. However, we make similar conclusions using other combinations; for instance, $\theta_1=117^\circ$ and $\theta_2=170^\circ$, $\theta_1=118^\circ$ and $\theta_2=170^\circ$, or $\theta_1=119^\circ$ and $\theta_2=170^\circ$. Our fixed-angle approach using $\nu_p$ and $\nu_t$ is a candidate method to determine $b_{bp}(\lambda)$ and $b_b(\lambda)$. It will surely be useful in the study of marine optics and in ocean color remote sensing applications.


## Funding Information

Japan Society for the Promotion of Science (JSPS KAKENHI); 15K05290
Deutscher Akademischer Austauschdienst Dienst (DAAD); A0604137


**Appendix A: Notations**

| | |
|---|---|
| $D$ | Diameter of particle (μm) |
| $E(\lambda)$ | Irradiance (W/m$^2$) |
| N | Number of data points |
| $N(D)$ | Number of particles for a given $D$ |
| $P(\theta,\lambda)$ | Phase function by bulk VSF (sr$^{-1}$) |
| $P_p(\theta,\lambda)$ | Phase function by particulate VSF (sr$^{-1}$) |
| $P_{p,avg}(\theta,\lambda)$ | Average of $P_p(\theta,\lambda)$ |
| $Q_p(\theta,\lambda)$ | Contribution of $\beta_p(\theta\pm\Delta\theta,\lambda)$ into $b_{bp}(\lambda)$ |
| $Q_{p,avg}(\theta,\lambda)$ | Average of $Q_p(\theta,\lambda)$ |
| $R(\theta_1,\theta_2)$ | Ratio of bulk scattering: $\beta(\theta_2,\lambda)/\beta(\theta_1,\lambda)$ |
| $R_{avg}(\theta_1,\theta_2)$ | Average of $R(\theta_1,\theta_2)$ |
| $R_p(\theta_1,\theta_2)$ | Ratio of particulate scattering: $\beta_p(\theta_2,\lambda)/\beta_p(\theta_1,\lambda)$ |
| $R_{p,avg}(\theta_1,\theta_2)$ | Average of $R_p(\theta_1,\theta_2)$ |
| $R_p^*(\theta_1,\theta_2)$ | Ratio of $Q_p(\theta,\lambda)$: $Q_p(\theta_2,\lambda)/Q_p(\theta_1,\lambda)$ |
| $b_b(\lambda)$ | Total backscattering coefficient (m$^{-1}$) |
| $b_{b,integral}(\lambda)$ | $b_b(\lambda)$ determined by the integration of $\beta(\theta,\lambda)$ |
| $b_{b,\nu t}(\lambda)$ | $b_b(\lambda)$ estimated using $\nu_t[R(\theta_1,\theta_2)]$ |
| $b_{b,\chi t}(\lambda)$ | $b_b(\lambda)$ estimated using $\chi_t(\theta)$ |
| $b_{bp}(\lambda)$ | Particulate backscattering coefficient (m$^{-1}$) |
| $b_{bp,freda}(\lambda)$ | $b_{bp}(\lambda)$ estimated using Freda's relation of $\varphi_p(140,\lambda)$ |
| $b_{bp,integral}(\lambda)$ | $b_{bp}(\lambda)$ determined by the integration of $\beta_p(\theta,\lambda)$ |
| $b_{bp,\nu p}(\lambda)$ | $b_{bp}(\lambda)$ estimated using $\nu_p[R_p(\theta_1,\theta_2)]$ |
| $b_{bp,\chi p}(\lambda)$ | $b_{bp}(\lambda)$ estimated using $\chi_p(\theta)$ |
| $b_{bsw}(\lambda)$ | Backscattering coefficient by seawater (m$^{-1}$) |
| $dI(\theta,\lambda)$ | Scattered intensity (W/sr) |
| $dv$ | Scattering volume (m$^3$) |
| $m$ | Complex refractive index relative to water |
| $n$ | Real part of the complex refractive index |
| $\beta(\theta,\lambda)$ | Bulk VSF (m$^{-1}$ sr$^{-1}$) |
| $\beta_p(\theta,\lambda)$ | VSF by suspended particles (m$^{-1}$ sr$^{-1}$) |
| $\beta_{sw}(\theta,\lambda)$ | VSF by pure seawater (m$^{-1}$ sr$^{-1}$) |
| $\theta$ | Scattering angle |
| $\kappa$ | Imaginary part of the complex refractive index |
| $\lambda$ | Wavelength (nm) |
| $\nu_p[R_p(\theta_1,\theta_2)]$ | Universal conversion factor related to $b_{bp}(\lambda)$ |
| $\nu_{p,avg}[R_p(\theta_1,\theta_2)]$ | Average of $\nu_p[R_p(\theta_1,\theta_2)]$ |
| $\nu_t[R(\theta_1,\theta_2)]$ | Universal conversion factor related to $b_b(\lambda)$ |
| $\xi$ | Junge exponent |
| $\sigma$ | Standard deviation |
| $\sigma^*$ | Standard deviation relative to mean value |
| $\varphi_p(\theta,\lambda)$ | Scaling factor related to $b_{bp}(\lambda)$ |
| $\varphi_{p,avg}(\theta,\lambda)$ | Average of $\varphi_p(\theta,\lambda)$ |
| $\varphi_{sw}(\theta,\lambda)$ | Scaling factor related to $b_{bsw}(\lambda)$ |
| $\varphi_t(\theta,\lambda)$ | Scaling factor related to $b_b(\lambda)$ |
| $\chi_p(\theta)$ | Conventional conversion factor related to $b_{bp}(\lambda)$ |
| $\chi_{p,avg}(\theta)$ | Average of $\chi_p(\theta)$ |
| $\chi_{p,literature}(\theta)$ | $\chi_p(\theta)$ values reported by previous studies |
| $\chi_{p,mean}(\theta)$ | Average over all $\chi_{p,literature}(\theta)$ |
| $\chi_{sw}(\theta)$ | Conventional conversion factor related to $b_{bsw}(\lambda)$ |
| $\chi_t(\theta)$ | Conventional conversion factor related to $b_b(\lambda)$ |
| PSD | Particle Size Distribution |
| RMSE | Root Mean Square Error |
| VSF | Volume Scattering Function |
| iVSFM | imaging Volume Scattering Function Meter |

**Appendix B: Range of the particulate beam attenuation coefficient (m$^{-1}$) for the samples we measured.**

| Types of waters | samples | min | max |
|---|---|---|---|
| Natural waters | River Elbe | 17.18 | 23.91 |
| | Lake Shaalsee | 0.35 | 2.52 |
| *Cultures* | *P. minimum* | 0.14 | 0.90 |
| | *R. baltica* | 0.19 | 1.06 |
| | *Synechococcus sp.* | 0.31 | 1.92 |
| | *Nannochloropsis sp.* | 0.12 | 1.73 |
| | *T. weissflogii* | 0.19 | 1.27 |

**Appendix C: $\chi_{p,literature}$ at 120° and 140°, and carried out λ and location in the historic literature. Note that, $\chi_{p,mean}$ shows average of $\chi_{p,literature}$.**

| | $\chi_{p,literature}(\theta)$ | | |
|---|---|---|---|
| Observer and location | 120° | 140° | λ (nm) |
| Boss and Pegau, | 1.12 | 1.18 | 532 |

| | | | |
|---|---|---|---|
| different oceans [5] | | | |
| Sullivan and Twardowski, different oceans [6] | 1.10 | 1.17 | 658 |
| Berthon *et al.*, Northern Adriatic Sea [7] | 1.09 | 1.16 | 443,555 |
| Chami *et al.*, Black sea [10] | 1.29 | 1.21 | 555 |
| Chami *et al.*, *cultures* [10] | 1.13 | 1.30 | 550 |
| Whitmire *et al.*, *cultures* [11] | 1.13 | 1.20 | 443-620 |
| Freda, Southern Baltic sea [12] | 1.07 | 1.12 | 443-620 |
| Petzold, clear ocean, St. 7 [18] | 1.15 | 1.35 | 514 |
| clear ocean, St. 8 | 1.40 | 1.55 | 514 |
| clear ocean, St. 9 | 1.46 | 1.41 | 514 |
| coastal ocean, St. 5 | 1.31 | 1.17 | 514 |
| coastal ocean, St. 11 | 1.28 | 1.26 | 514 |
| turbid harbor, St 2200 | 1.11 | 1.26 | 514 |
| turbid harbor, St 2040 | 1.04 | 1.22 | 514 |
| turbid harbor, St 2240 | 1.08 | 1.25 | 514 |
| $\chi_{p,mean}(\theta)$ | 1.18 | 1.25 | |

**Appendix D: Coefficients of $\nu_p[R_p(\theta_1,\theta_2)]$ function, i.e., $\nu_p[R_p(\theta_1,\theta_2)]=A*EXP[B*R_p(\theta_1,\theta_2)]$, where $R_p(\theta_1,\theta_2)$ is $\beta_p(\theta_2)/\beta_p(\theta_1)$. $r^2$ is the coefficient of determination. Furthermore, average and relative standard deviation of $R_p(\theta_1,\theta_2)$ are provided in the table to show VSF shape variations.**

| $\theta_1$ | $\theta_2$ | A | B | $r^2$ | $R_{p,avg}$ | $\sigma^*(R_p)$ |
|---|---|---|---|---|---|---|
| 90° | | 0.7778 | 0.0838 | 0.8096 | 4.62 | 47.6 % |
| 100° | | 0.9345 | 0.0699 | 0.9125 | 5.66 | 50.5 % |
| 110° | | 1.0044 | 0.0650 | 0.9588 | 6.15 | 52.8 % |
| 115° | | 1.0861 | 0.0601 | 0.9588 | 6.63 | 51.9 % |
| 117° | | 1.0384 | 0.0619 | 0.9629 | 6.25 | 51.9 % |
| 118° | | 1.0312 | 0.0622 | 0.9634 | 6.17 | 51.1 % |
| 119° | 170° | 1.0715 | 0.0602 | 0.9631 | 6.47 | 52.2 % |
| 120° | | 0.9939 | 0.0636 | 0.9608 | 5.87 | 51.2 % |
| 121° | | 0.9478 | 0.0663 | 0.9577 | 5.56 | 51.0 % |
| 122° | | 0.9887 | 0.0636 | 0.9580 | 5.80 | 50.6 % |
| 130° | | 0.9845 | 0.0617 | 0.9275 | 5.59 | 49.3 % |
| 140° | | 0.8881 | 0.0621 | 0.7752 | 4.70 | 46.4 % |
| 150° | | 0.7550 | 0.0576 | 0.3845 | 3.58 | 41.3 % |
| 160° | | 0.6189 | 0.0078 | 0.0014 | 2.35 | 31.4 % |
| | 90° | 0.9249 | 0.3484 | 0.1452 | 1.28 | 16.7 % |
| | 100° | 1.0899 | 0.2687 | 0.0274 | 1.05 | 11.5 % |
| | 110° | 3.1061 | -0.7940 | 0.0504 | 0.97 | 7.3 % |
| | 130° | 0.3312 | 1.4149 | 0.2027 | 1.04 | 6.0 % |
| | 140° | 0.5022 | 0.8639 | 0.3737 | 1.22 | 11.3 % |
| | 150° | 0.6350 | 0.5193 | 0.5545 | 1.58 | 17.7 % |
| 120° | 160° | 0.7580 | 0.2717 | 0.7204 | 2.37 | 25.7 % |
| | 165° | 0.8434 | 0.1740 | 0.8912 | 3.09 | 34.3 % |
| | 166° | 0.8641 | 0.1514 | 0.9190 | 3.39 | 36.4 % |
| | 167° | 0.8903 | 0.1281 | 0.9362 | 3.77 | 39.0 % |
| | 168° | 0.9174 | 0.1029 | 0.9452 | 4.41 | 41.8 % |
| | 169° | 0.9500 | 0.0811 | 0.9562 | 5.16 | 45.6 % |
| | 170° | 0.9939 | 0.0636 | 0.9608 | 5.87 | 51.2 % |

**Appendix E: Historic VSFs used for the evaluation of the fixed-angle approaches. Average of $\chi_p(120)$ and $\nu_p[R_p(120,170)]$ are provided in the table for reference. Δ in the fifth column is mean deviations of $\nu_p[R_p(120,170)]$ from $\chi_p(120)$ in %.**

| Observer, carried out location and λ | N | $\chi_{p,avg}(\theta)$ | $\nu_{p,avg}[R_p(\theta_1,\theta_2)]$ | \|Δ\| |
|---|---|---|---|---|
| Petzold, clear, coastal and turbid oceans, 514 nm [16] | 8 | 1.23 | 1.18 | 4.0 % |
| Sokolov *et al.*, Black sea, 443-620 nm [17] | 4 | 1.13 | 1.07 | 5.3 % |
| Lee *et al.*, very turbid waters of Atlantic, 550 nm [18] | 60 | 1.13 | 1.12 | 2.0 % |
| Mankovsky and Haltrin, different oceans and lake Baykal, 520 nm [19,20] | 35 | 1.23 | 1.20 | 7.1 % |
| Overall dataset | 107 | 1.17 | 1.15 | 3.9 % |

**Appendix F: Coefficients of $\nu[R(\theta_1,\theta_2)]$ function, i.e., $\nu[R(\theta_1,\theta_2)]=A*EXP[B*R(\theta_1,\theta_2)]$, where $R(\theta_1,\theta_2)$ is $\beta(\theta_2)/\beta(\theta_1)$. $r^2$ is the coefficient of determination. Furthermore, average and relative standard deviation of $R(\theta_1,\theta_2)$ are provided in the table to show VSF shape variations.**

| $\theta_1$ | $\theta_2$ | A | B | $r^2$ | $R_{,avg}$ | $\sigma^*(R)$ |
|---|---|---|---|---|---|---|
| 90° | | 0.8322 | 0.0850 | 0.7381 | 4.00 | 44.4 % |
| 100° | | 0.9608 | 0.0729 | 0.8842 | 4.65 | 47.1 % |
| 110° | | 1.0023 | 0.0692 | 0.9513 | 4.85 | 48.8 % |
| 115° | | 1.0515 | 0.0652 | 0.9627 | 5.04 | 48.2 % |
| 117° | | 1.0132 | 0.0668 | 0.9654 | 4.82 | 48.6 % |
| 118° | | 1.0064 | 0.0670 | 0.9643 | 4.77 | 47.8 % |
| 119° | 170° | 1.0304 | 0.0659 | 0.9640 | 4.91 | 48.8 % |
| 120° | | 0.9743 | 0.0684 | 0.9602 | 4.58 | 48.2 % |
| 121° | | 0.9385 | 0.0707 | 0.9597 | 4.40 | 47.9 % |
| 122° | | 0.9660 | 0.0685 | 0.9558 | 4.52 | 47.5 % |
| 130° | | 0.9417 | 0.0675 | 0.9065 | 4.29 | 46.9 % |
| 140° | | 0.8529 | 0.0675 | 0.7414 | 3.69 | 44.7 % |
| 150° | | 0.7433 | 0.0622 | 0.3886 | 2.96 | 40.3 % |
| 160° | | 0.6427 | 0.0068 | 0.0012 | 2.10 | 30.9 % |
| | 90° | 0.9455 | 0.2988 | 0.1136 | 1.15 | 15.1 % |
| | 100° | 1.0608 | 0.2300 | 0.0219 | 0.99 | 10.0 % |
| | 110° | 1.5571 | -0.1630 | 0.0035 | 0.95 | 5.9 % |
| | 130° | 0.3689 | 1.2114 | 0.1493 | 1.06 | 4.6 % |
| | 140° | 0.5016 | 0.7992 | 0.2986 | 1.22 | 8.6 % |
| | 150° | 0.6054 | 0.5242 | 0.4774 | 1.51 | 13.5 % |
| 120° | 160° | 0.7173 | 0.2964 | 0.6897 | 2.09 | 20.7 % |
| | 165° | 0.8120 | 0.1899 | 0.8819 | 2.61 | 29.2 % |
| | 166° | 0.8357 | 0.1653 | 0.9124 | 2.82 | 31.5 % |
| | 167° | 0.8636 | 0.1403 | 0.9327 | 3.09 | 34.3 % |
| | 168° | 0.8942 | 0.1127 | 0.9440 | 3.54 | 37.5 % |
| | 169° | 0.9302 | 0.0883 | 0.9564 | 4.07 | 41.9 % |
| | 170° | 0.9743 | 0.0684 | 0.9602 | 4.58 | 48.2 % |

## References


1. C. D. Mobley, Light and Water: Radiative Transfer in Natural Waters, (Academic, San Diego, Calif., 1994).
2. H. R. Gordon, O. B. Brown, and M. M. Jacobs, "Computed relationships between the inherent and apparent optical properties of a flat homogeneous ocean, "Appl. Opt. **14**(2), 417-427 (1975).
3. T. Oishi, "Significant relationship between the backward scattering coefficient of sea water and the scatterance at 120˚," Appl. Opt. **29**(31), 4658-4665 (1990).
4. R. A. Maffione and D. R. Dana, "Instruments and methods for measuring the backward-scattering coefficient of ocean waters," Appl. Opt. **36**(24), 6057-6067 (1997).
5. E. Boss and W. S. Pegau, "Relationship of light scattering at an angle in the backward direction to the backscattering coefficient," Appl. Opt. **40**(30), 5503-5507 (2001).
6. J. M. Sullivan and M. S. Twardowski, "Angular shape of the oceanic particulate volume scattering function in the backward direction," Appl. Opt. **48**(35), 6811-6819 (2009).

7. J.-F. Berthon, E. Shybanov, M. E.-G. Lee, and G. Zibordi, "Measurements and modeling of the volume scattering function in the coastal northern Adriatic Sea," Appl. Opt. **46**(22), 5189-5203 (2007).
8. X. Zhang, E. Boss, and D. J. Gray, "Significance of scattering by oceanic particles at angles around 120 degree," Opt. Express **22**, 31329-31336 (2014).
9. Y. Jodai, T. Oishi, Y. Saruya, and M. Kishino, "Bypass method for estimating backward scattering coefficient," Ocean Optics XIII, 461-465 (1996).
10. M. Chami, E. Marken, J. J. Stamnes, G. Khomenko, and G. Korotaev, "Variaibility of the relationship between the particulate backscattering coefficient and the volume scattering function measured at fixed angles," J. Geophys. Res. 111, C05013, 1-10, doi: 10.1029/2005JC003230 (2006).
11. L. Whitmire, W. S. Pegau, L. K. Boss, E. Boss, and T. J. Cowles, "Spectral backscattering properties of marine phytoplankton cultures," Opt. Express **18**(14), 15073-15093 (2010).
12. W. Freda, "Spectral dependence of the correlation between the backscattering coefficient and the volume scattering function measured in the southern Baltic Sea," Oceanologia. **54**, 355-367 (2012).
13. N. G. Jerlov, Marine Optics (Elsevier, Amsterdam, 1976).
14. H. Tan, R. Doerffer, T. Oishi, and A. Tanaka, "A new approach to measure the volume scattering function," Opt. Express **21**, 18697-18711 (2013).
15. A. Morel, "Optical properties of pure water and pure sea water," *in Optical Aspects of Oceanography*, N. G. Jerlov and E. S. Neilsen, eds, (Academic, New York, 1974).
16. G. Fournier and J. L. Forand, "Analytic phase function for ocean water," Ocean Optics XII, J. S. Jaffe, ed., Proc., SPIE **2258**, 194-201 (1994).
17. T. J. Petzold, "Volume Scattering Functions for Selected Ocean Waters," Technical Report SIO 72-78 Scripps Institute of Oceanography, San Diego, Calif. (1972).
18. A. Sokolov, M. Chami, E. Dmitriev, and G. Khomenko, "Parameterization of volume scattering function of coastal waters based on the statistical approach," Opt. Express **18**(5), 4615-4636 (2010).
19. M. E. Lee, V. I. Haltrin, E. B. Shybanov, and A. D. Weidemann, "Light scattering phase function of turbid coastal waters measured in LEO-15 experiment in 2000," in OCEANS 2003 MTS-IEEE Conference Proceedings on CD-ROM, San Diego, California, September 22-26, ISBN: 0-933957-31-9; Holland Enterprises, Escondido, CA, USA, 2835-2841 (2003).
20. V. I. Mankovsky and V. I. Haltrin, "Phase Functions of Light Scattering Measured in Waters of World Ocean and Lake Baykal," in 2002 IEEE International Geoscience and Remote Sensing Symposium and the 24th Canadian Symposium on Remote Sensing, Toronto, Canada, June 24-28, Paper I2E09_1759 (2002).
21. V. I. Mankovsky and V. I. Haltrin, "Light Scattering Phase Functions Measured in Waters of Mediterranean Sea," in Proceedings OCEANS 2002 MTS-IEEE, Biloxi, Mississippi, USA, October 29-31, 4, 2368-2373 (2002).
22. M. I. Mishchcnko, J. W. Hovenier, and L. D. Travis, "Light scattering by nonsphcrical particles.Theory, measurements, and applications," San Diego: AcademicPress (2000).
23. A. Morel, "Diffusion de la lumière par les eaux der mer; rèsultats expèrimentaux et approach thèorique", In: Optics of the Sea, NATO AGARD, Lect. Ser. 61, (1973).
24. J. M. Sullivan, M. S. Twardowski, P. L. Donaghay, and S. A. Freeman, "Use of optical scattering to discriminate particle types in coastal waters," Appl. Opt. **44**, 1667-1680 (2005).
25. E. Aas, "Refractive index of phytoplankton derived from its metabolite composition," J. Plankton Res. **18**, 2223-2249 (1996).
26. M. Babin, A. Morel, V. Fournier-Sicre, F. Fell, and D. Stramski, "Light scattering properties of marine particles in coastal and open ocean waters as related to the particle mass concentration," Limnol. Oceanogr. **48**, 843-859, (2003).
27. O. Ulloa, S. Sathendranath, and T. Platt, "Effect of the particle-size distribution on the backscattering ratio in seawater," Appl. Opt. **33**, 7070-7077 (1994).
28. H. C. van de Hulst, "Light Scattering by Small Particles," John Wiley, Hoboken, N. J., (1957).
29. A. Bricaud, and A. Morel, "Light attenuation and scattering by phytoplanktonic cells: a theoretical modeling," Appl. Opt. **25**(4), 571-580 (1986).